

Supporting Information:
**“X-ray irradiation effects on Egyptian blue and
green pigments“**

Marie Godet*, Laurent Binet, Sebastian Schöder, Lucile Brunel-Duverger,
Mathieu Thoury and Loïc Bertrand*

E-mail: msgodet@gmail.com;loic.bertrand@ens-paris-saclay.fr

Contents

1 SEM-EDX characterization of EB_K and EG_K	S-3
1.1 Experimental parameters	S-3
1.2 Results	S-3
2 XRD characterization of EB_K and EG_K	S-6
2.1 Experimental parameters	S-6
2.2 Results	S-6
3 Synchrotron XRF characterization of EB_a1, EB_K, EG_a3 and EG_K	S-7
3.1 Experimental parameters	S-7
3.2 Results	S-8
4 Dose calculations	S-10
4.1 Calculation of the attenuation lengths λ_{EB} and λ_{EG}	S-10
4.2 Doses received by the samples	S-12
5 Additional EPR data for Egyptian green samples EG_a3 and EG_K	S-12
6 Paramagnetic species detected in Egyptian blue and green samples	S-17
References	S-17

1 SEM-EDX characterization of EB_K and EG_K

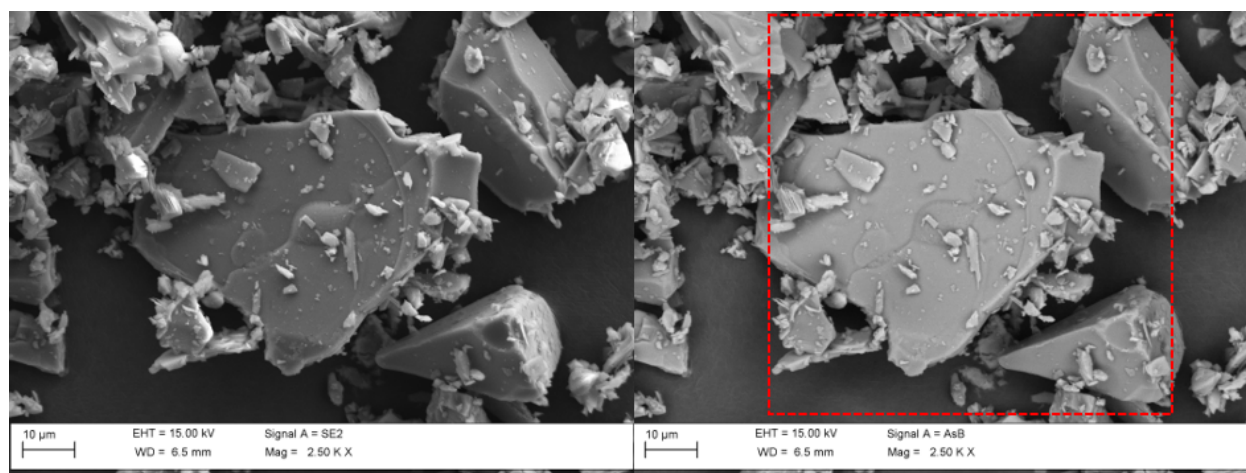
1.1 Experimental parameters

Crushed pigments powder were placed on a carbon tape and gold coated. SEM-EDX analysis was performed using a FEG ZEISS Supra55VP microscope coupled to a Bruker EDX detector. Spectral maps were acquired using the following parameters, excitation voltage: 15 kV, current: 60 μ m, high current mode, working distance: 6.5 mm, duration: 40 min, counts: 40 keV/90 kcps. Spectra were extracted from regions of interest and normalized to the intensity of the gold signal.

1.2 Results

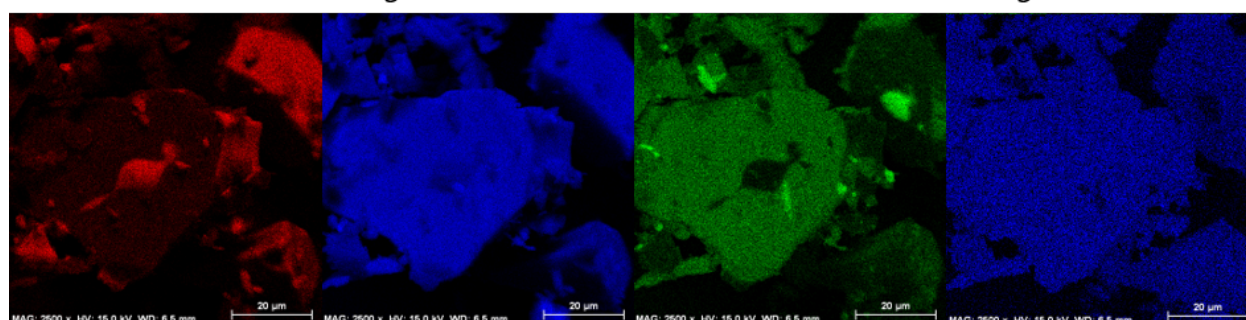
In EB_K, crushed blue particles show angular platelet shapes with sizes ranging from a few micrometers to a few tens of micrometers (Figure S1). Particles contain mostly O, Cu, Si, Ca (Sp 1), corresponding to the cuprorivaite $\text{CaCuSi}_4\text{O}_{10}$ detected by XRD. In addition, Ca-rich micro-particles are observed (Sp 2), corresponding to the wollastonite CaSiO_3 detected by XRD. Some areas containing mainly O, Cu, Na, Si and Mg, Al, Cl and Ca in small quantities are also observed (Sp 3), potentially corresponding to an amorphous phase or to a crystallized compound present in too small quantity to be detected by XRD.

In EG_K, crushed green particles have angular and irregular shapes with sizes ranging from a micrometer to a few tens of micrometers (Figure S2). Some regions contain mainly O, Cu, Na, Si, as well as Al in low concentration (Sp 1), probably corresponding to the amorphous phase (undetected by XRD) while others contain mainly O, Si (Sp 3), which correspond to the quartz and trydimite crystals detected by XRD. Small particles (less than 1 micrometer in size) containing O, Al and Si are also evidenced (Sp 2).



SEM-SE image

SEM-BSE image

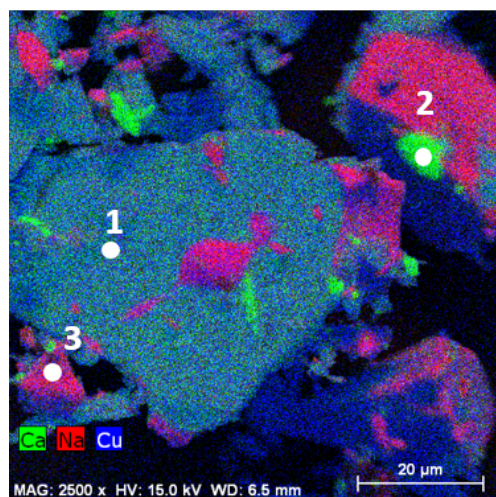


Na K

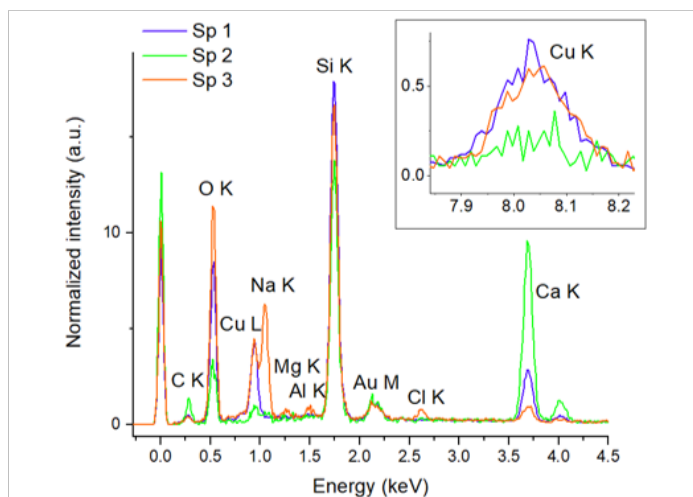
Si K

Ca K

Cu K

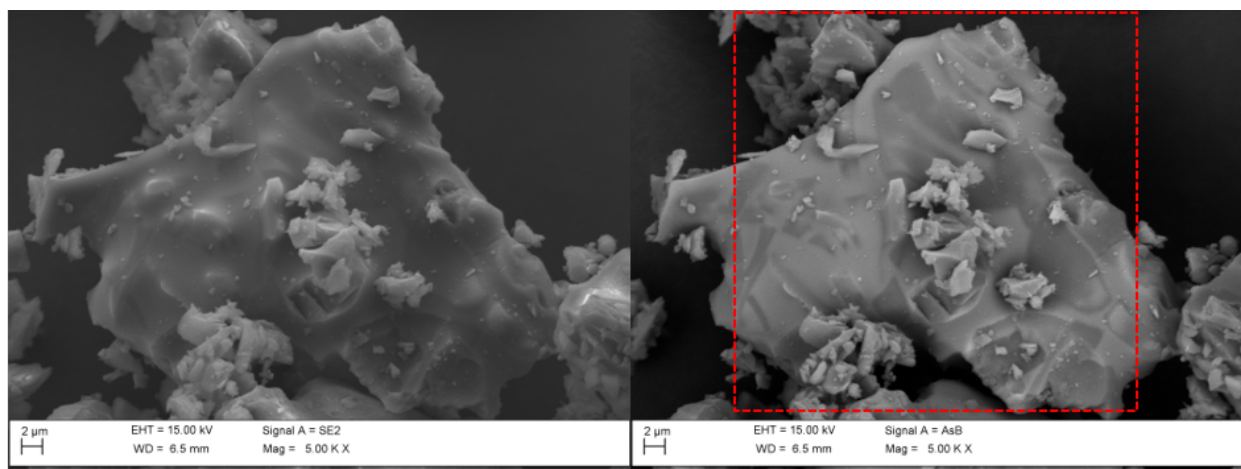


Superposition map Na Ca Cu



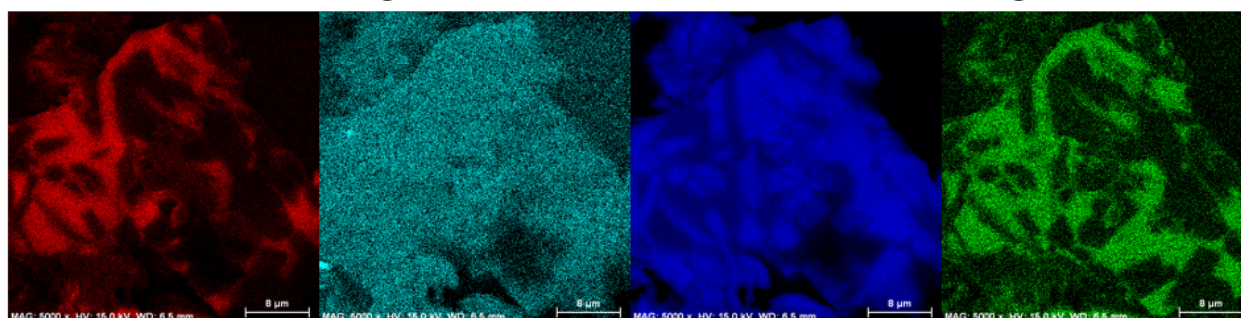
EDX spectra extracted from ROI and normalized

Figure S1: SEM-EDX analysis of EB_K; top: SEM imaging with localization of EDX analysis, middle: EDX maps for major elements except oxygen, bottom: EDX superposition map and spectra extracted from regions of interest indicated by numbers.



SEM-SE image

SEM-BSE image

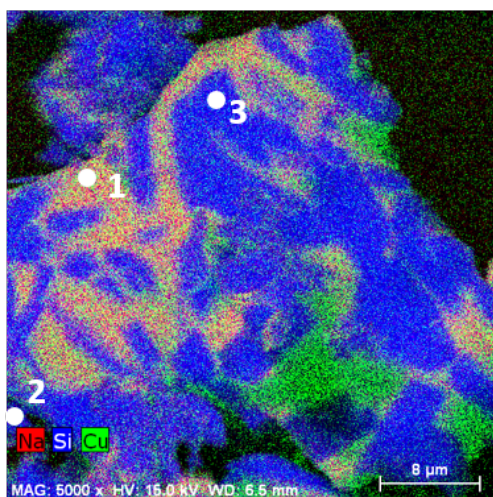


Na K

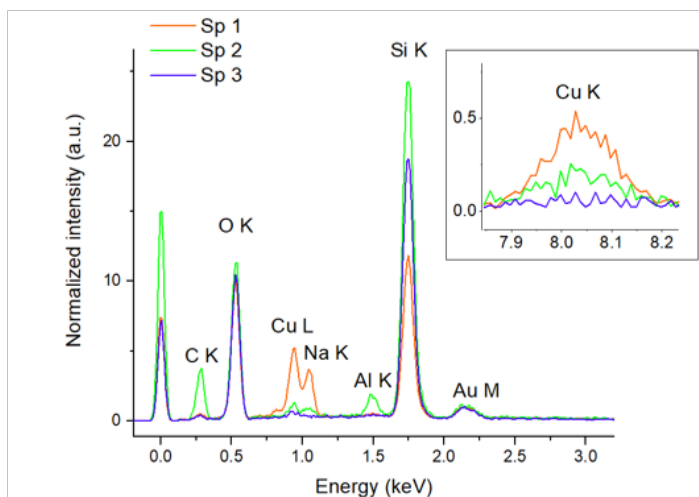
Al K

Si K

Cu K



Superposition map Na Si Cu



EDX spectra extracted from ROI and normalized

Figure S2: SEM-EDX analysis of EG_K; top: SEM imaging with localization of EDX analysis, middle: EDX maps for major elements except oxygen, bottom: EDX superposition map and spectra extracted from regions of interest indicated by numbers.

2 XRD characterization of EB_K and EG_K

2.1 Experimental parameters

Crushed pigments powders were analyzed using a diffractometer (X'Pert Pro, PANalytical) with a copper anode (Cu $K\alpha_1$, $\lambda = 1.5406 \text{ \AA}$) from 15° to 65° , step size: 0.03° , scan step time: 147.4 s and generator settings: 40 mA, 45 kV. Rietveld refinement was performed using the Fullprof software.

2.2 Results

XRD analysis indicates that EB_K contains mostly cuprorivaite $\text{CaCuSi}_4\text{O}_{10}$ (98 wt%) and wollastonite CaSiO_3 as a minor phase (2 wt%). For cuprorivaite, strong preferential orientation indicating “plate-like” crystals perpendicular to the c axis are evidenced (Figure S3). EB_K sample has a different microstructure than EB_a1 sample that contains quartz and trydimite as minor phases in addition to cuprorivaite (Pagès-Camagna, 1999).

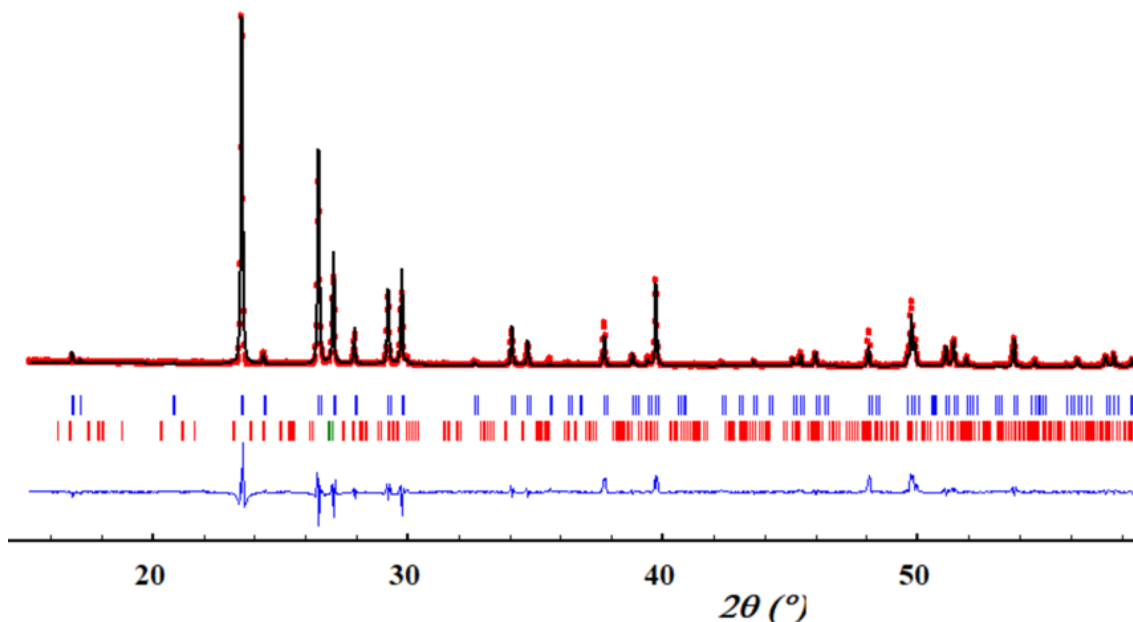


Figure S3: XRD analysis of the EB_K sample; blue: cuprorivaite $\text{CaCuSi}_4\text{O}_{10}$ (98 wt%), red: wollastonite CaSiO_3 (2 wt%), error = 2 %.

EG_K diffractogram shows mostly siliceous compounds such as trydimite SiO_2 and quartz SiO_2 (Figure S4). The amorphous phase was not detected. Sample EG_K has a different microstructure than sample EG_a3 which contains quartz and wollastonite in addition to the amorphous phase (Pagès-Camagna, 1999).

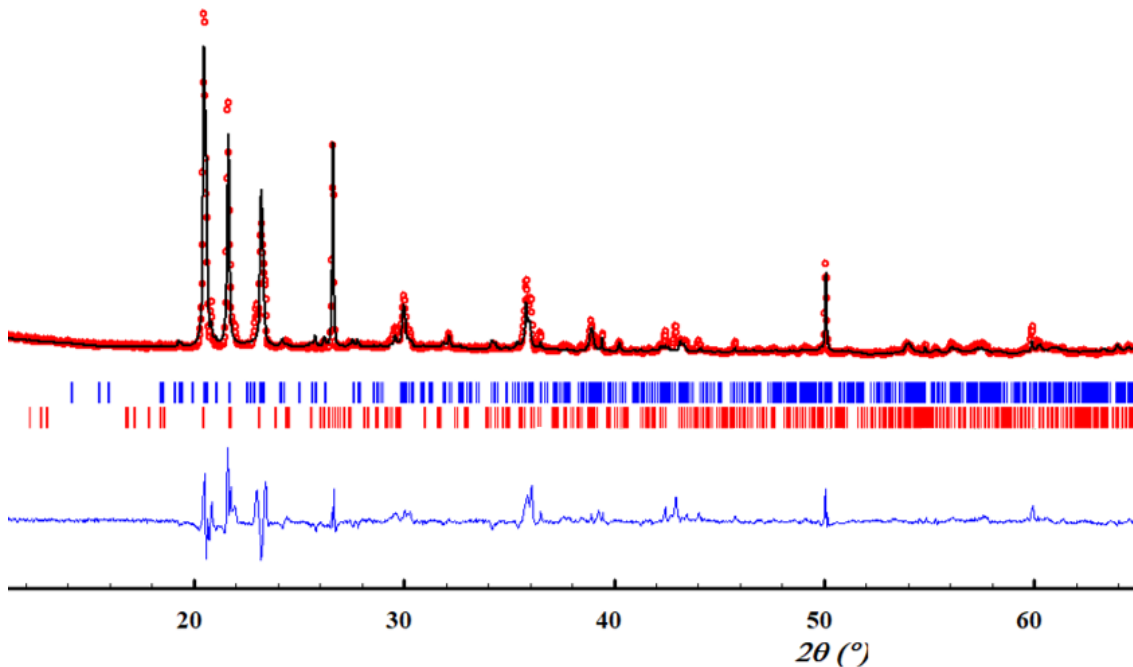


Figure S4: XRD analysis of the EG_K sample; blue: trydimite SiO_2 (80 wt%), red: quartz SiO_2 (15 wt%), error = 2 %.

3 Synchrotron XRF characterization of EB_a1, EB_K, EG_a3 and EG_K

3.1 Experimental parameters

XRF analysis was performed at the PUMA beamline of the Soleil synchrotron (Paris, France). Crushed pigments are placed in the sample-holders dedicated to irradiation, oriented at 45° to the beam ($S = 7000 \times 2800 \mu\text{m}^2$). Energy is scanned following this scan routine: 8800–8970 in 2 eV steps, 8970–9040 in 0.5 eV steps, 9040–9200 in 2 eV steps; 2.6 s per point.

The intensity is about $I = 1.1 \times 10^{10} \text{ ph}\cdot\text{s}^{-1}$ at 9 keV measured using a calibrated Si diode. The fluorescence signal is collected using an XRF Sirius-SD silicon drift detector (RaySpec Ltd) with an open active area of 80 mm^2 , $450 \mu\text{m}$ thick crystal and $25 \mu\text{m}$ thick Be window, positioned at 90° to the beam. The spectrometer has a resolution of 140 eV at 5.9 keV. The distance between the device and the sample was approximately 10 cm in macro-mode. After collection, XRF sum spectra were calculated using a code developed under the R statistical environment and displayed on Figure S5.

3.2 Results

Copper (Cu) is the major element detected in the four pigments. Calcium (Ca) is present in the two blue EB_a1 and EB_K, in the green EG_a3 and in trace amount in EG_K. Other elements including aluminum (Al), yttrium (Y), titanium (Ti) and barium (Ba) are detected as impurities. Al is detected in the four pigments, Y is detected in all the pigments except EG_K, Ti in all the pigments except EB_K. Elements originating from the beamline environment (investigated by recording a spectrum without the sample-holder) are argon (Ar), chromium (Cr), manganese (Mn), iron (Fe), nickel (Ni). Ca, Fe, Cu escape peaks are observed. Silicon (Si) sum peak is also visible in all the spectra except that of EB_K. These results are summarized in the Table S1.

Table S1: XRF analysis of Egyptian blue and green samples

Sample	Major elements	Minor elements
EB_a1	Ca, Cu	Al, Y, Ti
EB_K	Ca, Cu	Al, Y, Ba
EG_a3	Ca, Cu	Al, Y, Ti
EG_K	Cu	Al, Ca, Ti

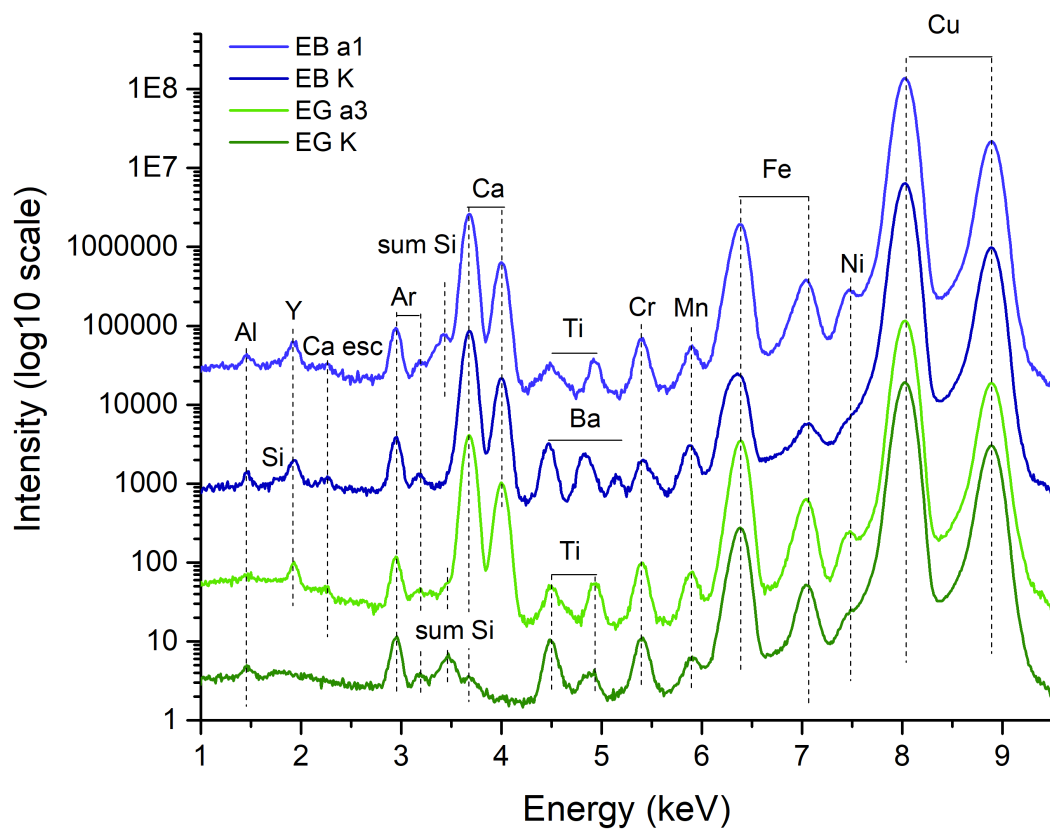


Figure S5: Synchrotron-based XRF analysis of Egyptian blue and green pigment samples; the spectra have been shifted vertically for easier visualisation.

4 Dose calculations

4.1 Calculation of the attenuation lengths λ_{EB} and λ_{EG}

To calculate the attenuation length λ_{EB} , Egyptian blue was modeled as pure cuprorivaite $\text{CaCuSi}_4\text{O}_{10}$ with a density $\rho_{\text{EB}} = 1.3 \text{ g}\cdot\text{cm}^{-3}$ (measured using commercial crushed pigment powder in graduated test tube). The value $\lambda_{\text{EB}} = \lambda_{\text{cupro}} \approx 170 \mu\text{m}$ was obtained using the online software by Henke et al.^{S1}.

Egyptian green was modeled as a weight mixture of quartz (SiO_2) $m_{\text{quartz}} = 0.7$ and wollastonite (CaSiO_3) $m_{\text{wolla}} = 0.3$. This proportion was obtained by averaging and normalizing the chemical composition of twenty Egyptian green pigments,^{S2} considering only the main elements Si, Ca and O. This proportion is converted in volumic concentration using $\rho_{\text{quartz}} = 2.65 \text{ g}\cdot\text{cm}^{-3}$,^{S3} $\rho_{\text{wolla}} = 2.84 \text{ g}\cdot\text{cm}^{-3}$ ^{S4} and the following equations:

$$m_{\text{wolla}} = \frac{M_{\text{wolla}}}{M_{\text{tot}}} = \frac{V_{\text{wolla}}}{V_{\text{wolla}} + \rho_{\text{quartz}} \times \frac{V_{\text{quartz}}}{\rho_{\text{wolla}}}} = 0.3$$

$$m_{\text{quartz}} = \frac{M_{\text{quartz}}}{M_{\text{tot}}} = \frac{V_{\text{quartz}}}{V_{\text{quartz}} + \rho_{\text{wolla}} \times \frac{V_{\text{wolla}}}{\rho_{\text{quartz}}}} = 0.7$$

We deduce

$$V_{\text{wolla}} = \frac{0.3 \times \rho_{\text{quartz}} \times V_{\text{quartz}}}{0.7 \times \rho_{\text{wolla}}} = 0.4 \times V_{\text{quartz}}$$

By replacing this expression in the volumic percentage formula, we obtain

$$v_{\text{wolla}} = \frac{V_{\text{wolla}}}{V_{\text{tot}}} = \frac{0.4 \times V_{\text{quartz}}}{1.4 \times V_{\text{quartz}}} = 0.29$$

and

$$v_{\text{quartz}} = \frac{V_{\text{quartz}}}{V_{\text{tot}}} = \frac{V_{\text{quartz}}}{1.4 \times V_{\text{quartz}}} = 0.71$$

The volume percentages values are similar to the weight one as the densities of the materials are very close. We then calculate the volume ratio $v = \frac{v_{\text{wolla}}}{v_{\text{quartz}}} = 0.29/0.71 = 0.41$ and the packing density x_i , defined as $x_i = \frac{\rho_{\text{EG}}}{\rho_{\text{tot}}} = 0.48$ with $\rho_{\text{EG}} = 1.3 \text{ g}\cdot\text{cm}^{-3}$ the density of the Egyptian green pigment powder (measured using the commercial crushed powder) and $\rho_{\text{tot}} = \frac{M_{\text{tot}}}{V_{\text{tot}}} = 0.95 \times \rho_{\text{wolla}} = 2.70 \text{ g}\cdot\text{cm}^{-3}$.

Supposing that the volume ratio v is equal to the linear ratio $v = l = \frac{l_{\text{wolla}}}{l_{\text{quartz}}}$, with l corresponding to the fraction of the beam path in the mixed media, we have the equation:

$$I = I_0 \times \exp^{-(l_{\text{wolla}} \cdot \mu_{\text{wolla}})} \times \exp^{-(l_{\text{quartz}} \cdot \mu_{\text{quartz}})} = I_0 \times \exp^{-(l_{\text{wolla}} \cdot \mu_{\text{wolla}} + l_{\text{quartz}} \cdot \mu_{\text{quartz}})}$$

We also have

$$I = I_0 \times \exp^{-(l_{\text{tot}} \cdot \mu_{\text{EG}})}$$

Thus

$$l_{\text{tot}} \times \mu_{\text{EG}} = l_{\text{wolla}} \times \mu_{\text{wolla}} + l_{\text{quartz}} \times \mu_{\text{quartz}}$$

As $l_{\text{tot}} = l_{\text{wolla}} + l_{\text{quartz}}$ and $v = l$, we deduce

$$\mu_{\text{EG}} = \frac{l_{\text{wolla}} \times \mu_{\text{wolla}} + l_{\text{quartz}} \times \mu_{\text{quartz}}}{l_{\text{wolla}} + l_{\text{quartz}}}$$

$$\mu_{\text{EG}} = \frac{v \times \mu_{\text{wolla}} + \mu_{\text{quartz}}}{v + 1}$$

By taking into account the packing density in the equation x_i , we obtain the Egyptian green powder absorption coefficient using $\mu_{\text{wolla}} = 61 \text{ cm}^{-1}$ and $\mu_{\text{quartz}} = 25 \text{ cm}^{-1}$.^{S5}

$$\mu_{\text{EG}} = x_i \times \frac{v \times \mu_{\text{wolla}} + \mu_{\text{quartz}}}{v + 1} = 17.1 \text{ cm}^{-1}$$

And finally the attenuation length λ_{EG}

$$\lambda_{\text{EG}} = \frac{1}{\mu_{\text{EG}}} \approx 0.059 \text{ cm} = 590 \mu\text{m}$$

4.2 Doses received by the samples

The doses received by each sample are summarized in table S2.

Table S2: Doses used to irradiate the samples (in MGy); the number in brackets corresponds to the irradiation session. For session 1, the dose rate values used are $D_{\text{EB}} = 321 \text{ Gy}\cdot\text{s}^{-1}$ and $D_{\text{EG}} = 109 \text{ Gy}\cdot\text{s}^{-1}$ and for session 2 the dose rate values are $D_{\text{EB}} = 184 \text{ Gy}\cdot\text{s}^{-1}$ and $D_{\text{EG}} = 62 \text{ Gy}\cdot\text{s}^{-1}$.

Irr. time	EB_K	EB_a1	EG_K	EG_a3
23 s			0.001 (2)	0.003 (1)
4 min	0.08 (1)	0.04 (2)	0.01 (2)	0.03 (1)
6 min			0.04 (1)	
20 min	0.4 (1)	0.2 (2)	0.12 (1)	0.1 (1)
38 min	0.7 (1)	0.4 (2)	0.14 (2)	0.3 (1)
1.5 hours			0.6 (1)	
2.1 hours	2.5 (1)			
10 hours		6.6 (2)		
11.5 hours	13 (1)			
11.5 hours				4.5 (1)
14.4 hours			3.2 (2)	
60 hours	69 (1)			

5 Additional EPR data for Egyptian green samples

EG_a3 and EG_K

The following EPR spectra illustrate the presence of various impurities in Egyptian green samples (section 3.2). For both samples, low-symmetry Fe^{3+} is detected at 30 K (displayed for EG_a3 on Figure S6). At 290 K, EPR spectra of modern green sample EG_K show a large signal corresponding to ferromagnetic particles impurities. Besides, in the sample irradiated

at 0.004 MGy and only at this dose, a first series transition ion impurity is observed at $g = 3.4$ (Figure S7). At 30 K, other transition ion impurities are detected in powder samples irradiated at various doses (displayed for instance at an irradiation dose of 0.1 MGy on Figure S8).

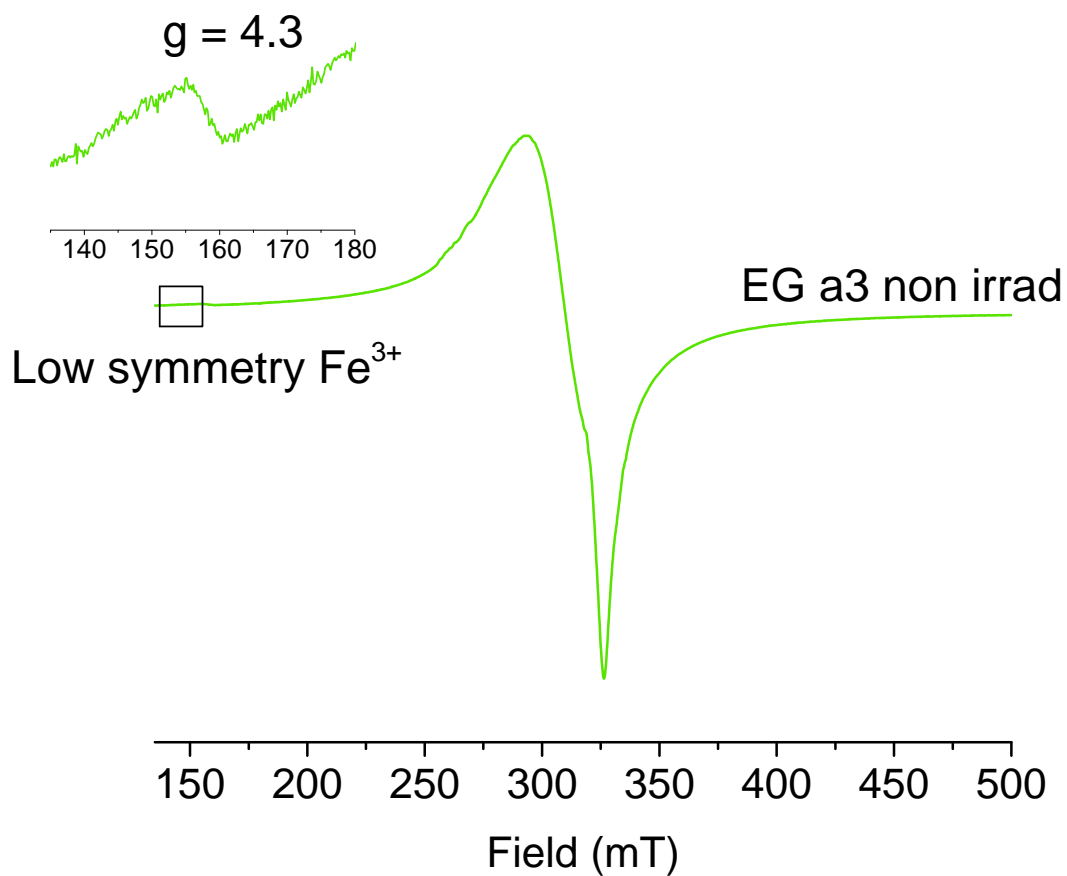


Figure S6: EPR spectrum of non-irradiated EG_a3 at 30 K showing the presence of Fe³⁺ impurity.

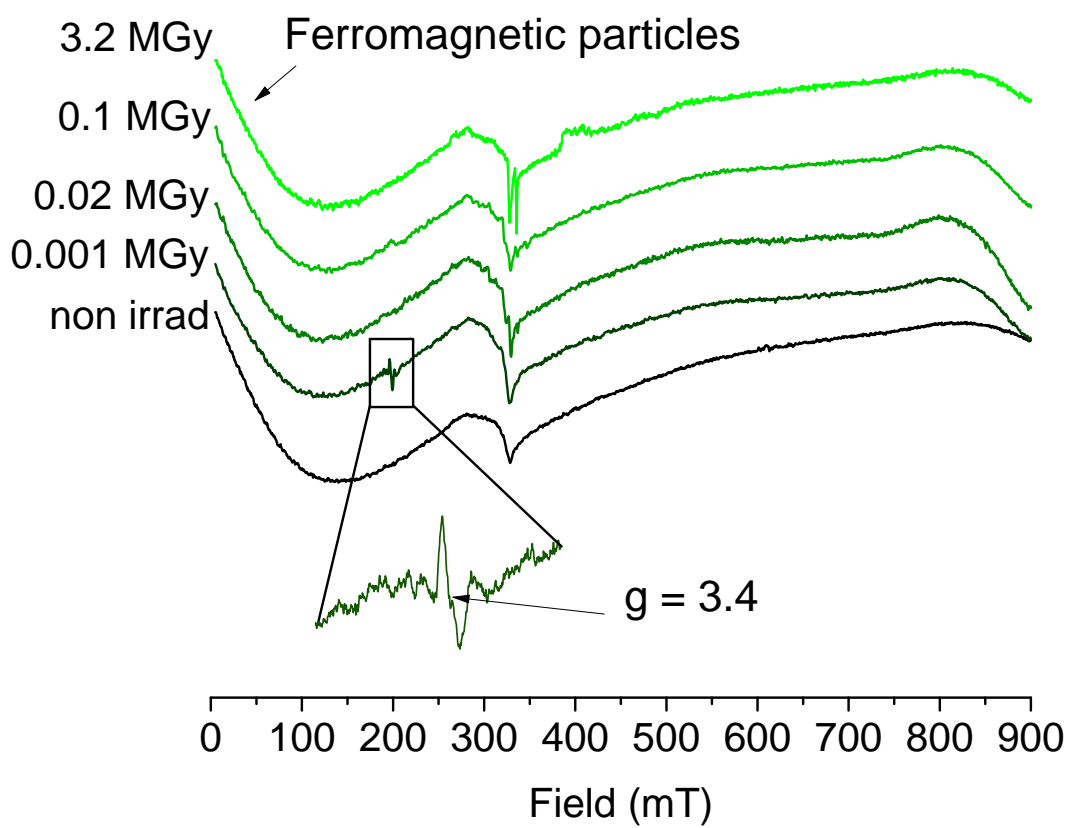


Figure S7: EPR spectra of EG.K at 290 K at increasing doses showing the presence of ferromagnetic particles and transition ion impurity at $g = 3.4$, possibly Fe^{2+} .

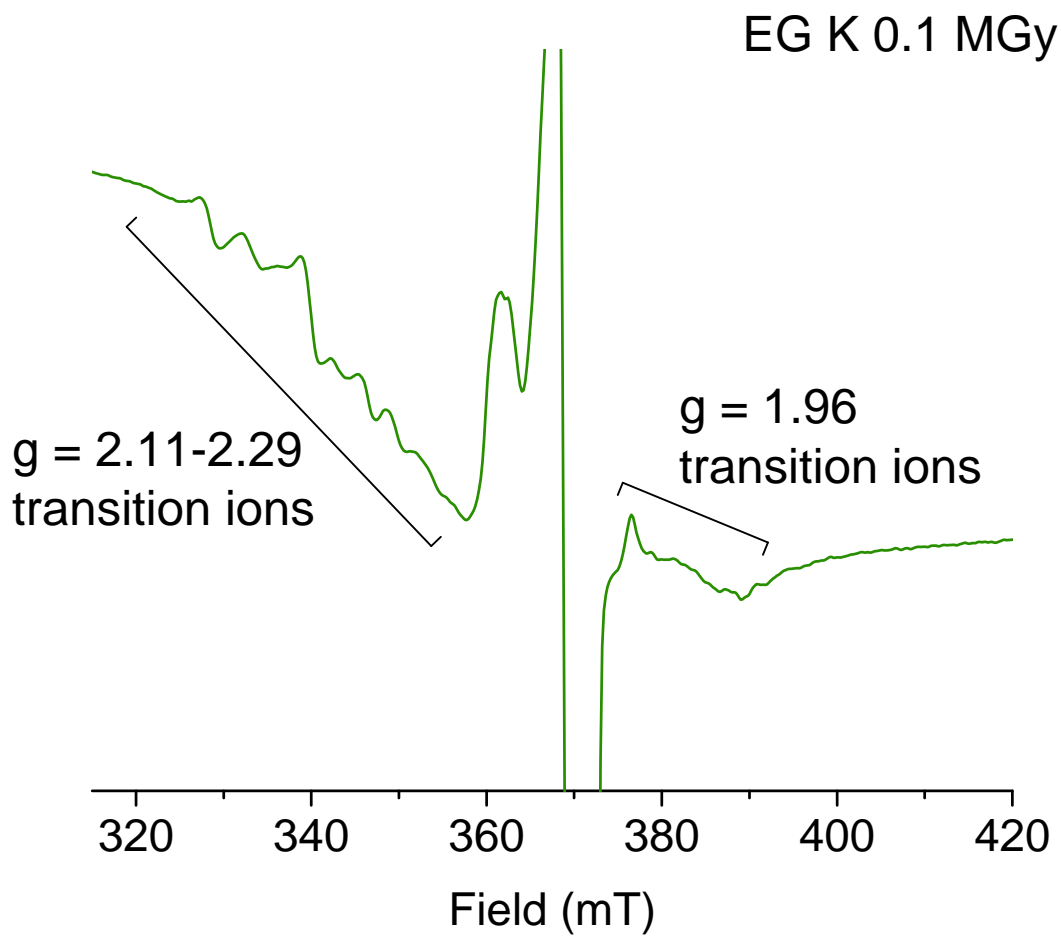


Figure S8: EPR spectrum of EG_K at 30 K irradiated at 0.1 MGy showing the presence of transition ion impurities at $g = 2.11 - 2.29$ and $g \approx 1.96$.

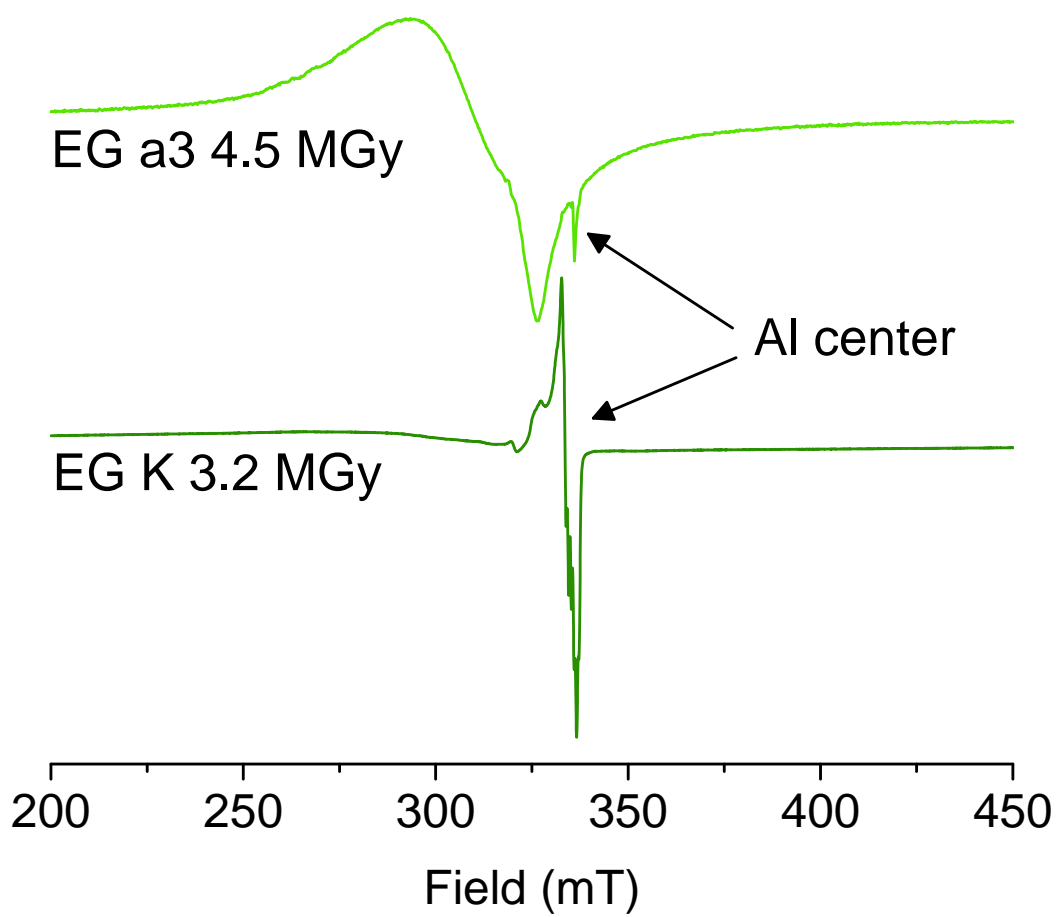


Figure S9: Al centers detected in Egyptian green samples after irradiation (30 K).

6 Paramagnetic species detected in Egyptian blue and green samples

The table S3 summarises the different paramagnetic impurities and radiation-induced defects detected in the Egyptian blue and green samples using EPR spectroscopy.

Table S3: Paramagnetic species in Egyptian blue and Egyptian green samples.

Sample	Transition ions	Radiation-induced defects	
		at 290 K	at 30 K
Arch. blue EB_a1	Cu^{2+} in $\text{CaCuSi}_4\text{O}_{10}$	E' ($g = 1.9986$)	E' ($g = 1.9994$), Al centers
Modern blue EB_K	Cu^{2+} in $\text{CaCuSi}_4\text{O}_{10}$	E' ($g = 1.9990$)	E' ($g = 1.9971$)
Arch. green EG_a3	Cu^{2+} in glass, Fe^{3+}	E' ($g = 2.0027$), OHC ($g = 2.0060$; $g = 2.0097$; $g = 2.0136$)	Al centers
Modern green EG_K	Cu^{2+} in glass, Fe^{3+} , ferromagnetic particles, transition ion impurities	E' ($g_{\parallel} = 2.0014$, $g_{\perp} = 2.0005$), E' ($g = 2.0016$)	Al centers

References

- (S1) Henke, B. L.; Gullikson, E. M.; Davis, J. C. X-ray interactions: photoabsorption, scattering, transmission and reflection $E = 50\text{--}30,000$ eV, $Z = 1\text{--}92$. *Atomic Data and Nuclear Data Tables* **1993**, *54*, 181–342.
- (S2) Hatton, G. D.; Shortland, A. J.; Tite, M. S. The production technology of Egyptian blue and green frits from second millennium BC Egypt and Mesopotamia. *Journal of Archaeological Science* **2008**, *35*, 1591–1604.

- (S3) Webmineral, Quartz Mineral Data. <http://webmineral.com/data/Quartz.shtml>, Accessed: 2021-08-18.
- (S4) Webmineral, Wollastonite-1A Mineral Data. <http://www.webmineral.com/data/Wollastonite-1A.shtml>, Accessed: 2021-08-18.
- (S5) National Institute of Standards and Technology, X-ray form factor, attenuation and scattering tables. <https://physics.nist.gov/PhysRefData/FFast/html/form.html>, Accessed: 2021-08-18.